International Journal of Thermophysics, Vol. 12, No. 1, 1991

High-Temperature Thermal Conductivity of $NdCoO_3$ and $GdCoO_3$

C. G. S. Pillai[1] **and A. M. George**[1]

Received November 21, 1989

Thermal conductivity of $NdCoO_3$ and $GdCoO_3$ has been studied from 300 to 1200 K. The conductivity is mainly excitonic, arising from the interactions of the t_{2g}–e_g states of cobalt ions in the oxides and shows characteristic maxima at 1030 and 975 K, respectively, corresponding with their semiconductor–metal transition temperatures. Contributions to thermal conductivity by phononic, electronic, ambipolar, and excitonic modes of conduction are calculated from measured thermal and electrical conductivity data in this temperature range. The energy of exciton formation in both the compounds is found to be 0.11 eV, same as in the case of $LaCoO_3$.

KEY WORDS: exciton formation energy; $GdCoO_3$; $NdCoO_3$; thermal conductivity.

1. INTRODUCTION

Busch and Schneider [1], while studing the thermal conductivity of InSb, observed an anomalous increase in the conductivity above 373 K instead of the characteristic decrease with temperature. They further noted that the conductivity excess, i.e., the difference between the measured conductivity and the extrapolated phononic part, involves an activation process and varies exponentially with temperature. Subsequently, Joffe [2], during his investigations on heat transfer in semiconductors, verified the phenomenon in a number of materials such as PbTe, Ge, HgTe, etc. After detailed study of the semiconducting properties and thermal resistivity of PbTe, he concluded that heat carriers in these materials are mainly excitons. In order to elicit support for the exciton hypothesis, he surveyed the absorption spectra of some of the compounds, but no concrete evidence could be obtained.

[1] Chemistry Division, Bhabha Atomic Research Center, Bombay-400085, India.

0195-928X/91/0100-0207$06.50/0

Meanwhile, Devyatkova [3] observed a similar increase in the thermal conductivity of certain minerals which also could not be accounted for by the classical mechanisms.

Pikus [4] carried out theoretical calculations on thermal conduction by excitons relating their effective mass, mean free path, and energy of formation. However, due to lack of thermal conductivity data on materials wherein existence of exciton states has been established, the excitonic mode of heat conduction remains ambiguous in literature.

Rare earth cobalt oxides, $RECoO_3$ (RE = La, Nd, and Gd) are typical examples of perovskites showing the simultaneous presence of high- and low-spin cobalt +3 valence states [5, 6]. Due to the temperature-depenent spin transitions, they exhibit a wide variety of electrical and magnetic properties and have been extensively investigated [7–12]. Raccah and Goodenough [7] have shown that in $LaCoO_3$, as the temperature is raised the low-spin $Co^{III}(t_{2g}^6)$ passes over to the high-spin $Co^{+3}(t_{2g}^4 e_g^2)$ state up to a certain temperature, above which the ions distribute themselves into both the low-spin Co^{IV} and the high-spin Co^{+2} states. In either processes the formation of excitons due to coupling of the e_g electron with the t_{2g} hole is associated. The compound undergoes a first-order semiconductor-to-metal transition at 1210 K due to the transfer of electrons to the collective σ^* band. Subsequently Bhide et al. [8] and Rajoria et al. [9] have noted that in $NdCoO_3$ and $GdCoO_3$, the thermal interactions of the Co-spin states are more or less similar, although, unlike in $LaCoO_3$, the ordering of the low- and high-spin Co ions in the sublattices are very weak. Semiconductor–metal/semimetal transitions are observed in these compounds at 1030 and 970 K, respectively.

Gerthsen and Kettle [13] studied the thermal conductivity of $LaCoO_3$, $NdCoO_3$, and Th and Sr doped ones from 140 to 750 K. Below 300 K, the conductivity decreases linearly with the inverse of temperature typical of a phononic conductor. However, above 300 K the conductivity is found to increase rapidly. From their data on the Seebeck coefficient and electrical conductivity, they explained the anomalous increase in the thermal conductivity in terms of the contribution of excitons. Subsequently, we have confirmed the existence of the excitonic mode of thermal conduction in $LaCoO_3$ [14]. A maximum in thermal conductivity is observed at 1210 K, coinciding with the semiconductor-to-metal transition temperature [15, 16].

The paper presents and discusses results of studies on these materials in order to improve the understanding of this interesting property of rare earth cobalt oxides. Measurements of thermal conductivity have been made to 1200 K on $NdCoO_3$ and $GdCoO_3$, well above their reported semiconductor–metal transition temperatures. In the case of $GdCoO_3$ its thermal conductivity has not been reported in the literature so far.

2. EXPERIMENTAL

The compounds $NdCoO_3$ and $GdCoO_3$ were prepared by solid-state reactions of fine mixtures of the rare earth oxide and $CoCO_3$ having a purity >99.9%, in the required stoichiometry. The reactants were ground throughly and the mixture was initially heated at 1000 K in air for a period of 10 h. The product was then ground and reheated at 1400 K for a further period of 10 h. The processes were repeated a few times to ensure the completion of the reaction. The compounds were characterized by XRD using Ni-filtered CuK_α radiation.

Sintered samples for the measurements were prepared by uniaxial cold compaction of the powder followed by sintering overnight at 1500 K in air. The sintered blocks or pellets were thereafter annealed at 1200 K for 48 h and shaped to the required dimensions (2.5 cm in diameter and ~2.5 cm in height for thermal conductivity and 1.2 cm in diameter and ~2 mm in thickness for electrical conductivity) by lapping. The bulk densities of the samples varied between 70 and 90% of the theoretical density.

The thermal conductivity of the samples was measured in air by the comparative method. The details of the equipment have been described elsewhere [16, 17]. The arrangement of the column of sample, references, etc., for the measurement was similar to that employed by Mirkovich [18]. The important modifications were that an auxiliary heater was inserted (for better control of heat flow in the column) between the heat sink and the standard, and both the heat source and the auxiliary heater were flat heaters of the same diameter as the sample and standard. They were fabricated by embedding coiled Kanthal resistive heating wire in alumina cement. The entire stack is clamped in a rigid frame with spring loading, employing about 1000–5000 N, and introduced into the guard furnace. Stabilized DC power was used for energizing the heat source. The temperatures of the guard furnace having four independent heaters were controlled to 0.1 K using platinum/platinum–13% rhodium thermocouples; temperature of each heater was monitored. The temperatures of the sample column were measured at eight points with 28 SWG Chromel/Alumel thermocouples; the thermocouple beads inserted into holes on the sample, references, and heat stabilizers.

The interfacial thermal resistance was kept minimal by interposing thin foils of platinum (0.01 mm thick) between the finely polished contacting surfaces.

Pyroceram-9606 and Inconel-718 thermal conductivity reference materials obtained from M/s. Dynatech Corporation, U.S.A., were used as standards for the measurements. The measurements were carried out in the temperature range 300–1200 K on at least two samples in each case. The overall accuracy of the measurements was better than ±5%.

Table I. Measured Values of Thermal Conductivity of $NdCoO_3$ and $GdCoO_3$

Sample density	Inconel-718[a] Temp. (K)	Inconel-718[a] λ ($W \cdot m^{-1} \cdot K^{-1}$)	Pyroceram-9606[a] Temp. (K)	Pyroceram-9606[a] λ ($W \cdot m^{-1} \cdot K^{-1}$)
		$NdCoO_3$		
I, 80% TD[b]	367	2.90	330	2.88
	400	2.88	393	3.19
	414	3.04	458	3.60
	464	3.44	527	4.00
	500	3.60	590	4.79
	548	3.86	685	6.02
	591	4.60	796	6.82
	640	5.50	862	7.60
	708	6.02	947	8.40
	767	6.39	1042	8.80
	820	7.03	1140	7.60
	857	7.60		
	935	8.38		
	992	9.19		
	1039	9.21		
	1084	9.04		
	1149	7.61		
	1192	6.41		
II, 71.5% TD	377	2.63	324	2.70
	415	2.69	360	2.80
	467	3.20	408	2.90
	516	3.20	460	3.10
	580	3.86	495	3.30
	622	4.29	530	3.50
	684	4.73	585	4.00
	752	5.36	631	4.31
	810	6.00	701	5.00
	884	6.78	744	5.50
	962	7.86	810	6.19
	1015	8.21	854	6.82
	1042	8.25	903	7.29
	1066	8.25	945	7.99
	1122	7.44	1009	8.32
	1176	6.07	1056	8.45
			1093	8.01
			1145	6.50
			1210	4.93

[a] Reference material.
[b] Theoretical density.

Table I. (*Continued*)

		$GdCoO_3$		
I, 85% TD	340	3.02	370	2.55
	437	3.40	463	2.98
	552	5.10	590	5.48
	670	6.02	650	6.00
	890	8.50	750	6.98
	940	9.34	837	7.24
	994	9.18	920	8.89
	1050	8.62	967	9.35
	1150	6.80	1023	8.51
			1086	7.60
			1107	7.40
II, 80% TD	368	2.90	353	2.96
	488	3.76	445	3.44
	524	4.09	550	4.56
	584	4.80	620	5.26
	675	5.68	792	7.02
	715	6.18	866	7.67
	905	8.18	993	8.49
	956	8.76	1037	8.01
	1012	8.49	1131	6.58
	1197	5.25	1203	5.29

The electrical conductivity of the samples was measured using a four-probe DC cell [19]. The measurement, besides supplying the required data for further calculation, was found to provide an excellent method to characterize the samples by their intrinsic properties.

3. RESULTS

The experimental results obtained on two samples for each oxide are given in Table I. Their conductivity increases rapidly with a rise in temperature, reaches a maximum, and falls thereafter; the maxima observed are at 1030 and 975 K for $NdCoO_3$ and $GdCoO_3$, respectively. The data were corrected for porosity using the simplified equation of Leob [20]:

$$\lambda = \lambda_0(1 - \phi) \tag{1}$$

where λ is the measured thermal conductivity, λ_0 is that for the material with zero porosity, and ϕ is the volume pore fraction. The variation of their corrected thermal conductivity with temperature is shown in Fig. 1. The data we obtained previously on $LaCoO_3$ [15] are also shown for comparision. Our data on $NdCoO_3$ are in good agreement with those of Gerthsen

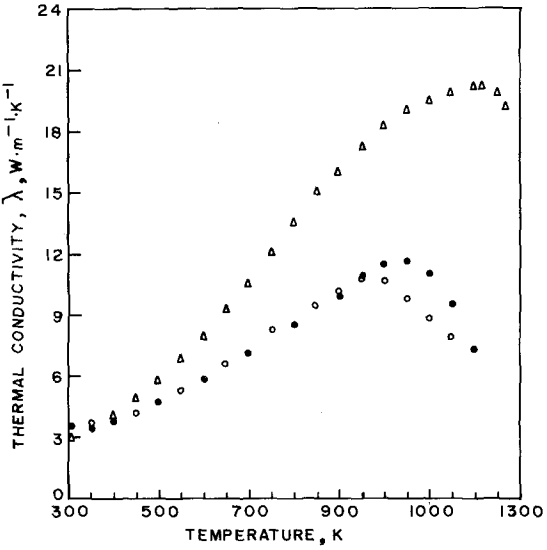

Fig. 1. Thermal conductivity (corrected for porosity) of $NdCoO_3$ (●), $GdCoO_3$ (○), and $LaCoO_3$ (△) versus temperature.

and Kettle [13], though slightly on the higher side in the respective temperature interval of 300 to 750 K. This deviation might have resulted from the lower densities of their samples used for the measurements as noted in the case of $LaCoO_3$ [14] and is eliminated if their sample densities are assumed to be 65% of theoretical value.

The measured electrical conductivity values of these oxide specimens are given in Table II. The logarithm of the electrical conductivity of the oxides versus inverse absolute temperature is given in Fig. 2. The data are in good agreement with those reported in the literature [9, 11]. The conductivity values were least-square fitted to the equation:

$$\sigma = \sigma_0 \exp(-\Delta E/kT) \tag{2}$$

where σ_0 is the characteristic constant, ΔE is the activation energy for electrical conduction, k is Boltzmann's constant, and T is the absolute temperature. The following linear expressions were obtained (in $\Omega^{-1} \cdot m^{-1}$):

$$\log_e \sigma\langle NdCoO_3\rangle$$

$$= (11.426 - 3828/T) \pm 0.071 \quad \text{for} \quad 300 \leqslant T \leqslant 450 \text{ K} \tag{3}$$

$$= (19.085 - 7270/T) \pm 0.022 \quad \text{for} \quad 450 \leqslant T \leqslant 800 \text{ K} \tag{4}$$

$$= (11.642 - 1280/T) \pm 0.035 \quad \text{for} \quad 850 \leqslant T \leqslant 1250 \text{ K} \tag{5}$$

$$\log_e \sigma\langle GdCoO_3\rangle$$

$$= (6.940 - 2614/T) \pm 0.085 \quad \text{for} \quad 300 \leqslant T \leqslant 450\ \text{K} \tag{6}$$

$$= (19.735 - 8599/T) \pm 0.017 \quad \text{for} \quad 500 \leqslant T \leqslant 800\ \text{K} \tag{7}$$

$$= (10.888 - 1027/T) \pm 0.024 \quad \text{for} \quad 850 \leqslant T \leqslant 1250\ \text{K} \tag{8}$$

Table II. Measured Values of Electrical Conductivity (σ) of $NdCoO_3$ and $GdCoO_3$

$NdCoO_3$		$GdCoO_3$	
Temp. (K)	$\sigma \times 10^{-2}$ ($\Omega^{-1} \cdot m^{-1}$)	Temp. (K)	$\sigma \times 10^{-2}$ ($\Omega^{-1} \cdot m^{-1}$)
295	0.002	300	0.002
310	0.004	325	0.004
335	0.010	350	0.006
355	0.018	375	0.010
385	0.042	400	0.013
400	0.056	415	0.020
415	0.100	450	0.032
450	0.200	475	0.061
470	0.631	500	0.126
475	0.316	525	0.398
495	0.725	575	0.903
510	1.002	600	1.567
520	1.584	610	2.243
530	1.950	625	4.000
555	4.693	650	6.098
590	7.758	675	10.470
625	17.95	700	15.85
680	50.30	725	25.13
715	70.96	750	44.66
735	99.89	770	56.63
750	149.61	775	63.09
780	125.75	800	91.24
840	258.50	825	133.40
875	254.13	875	158.90
905	281.77	910	178.60
925	282.56	925	175.00
965	298.50	975	191.10
1000	316.96	1025	202.80
1030	316.25	1075	204.20
1090	355.70	1125	209.10
1200	375.80	1175	221.29
1250	447.70	1250	237.10

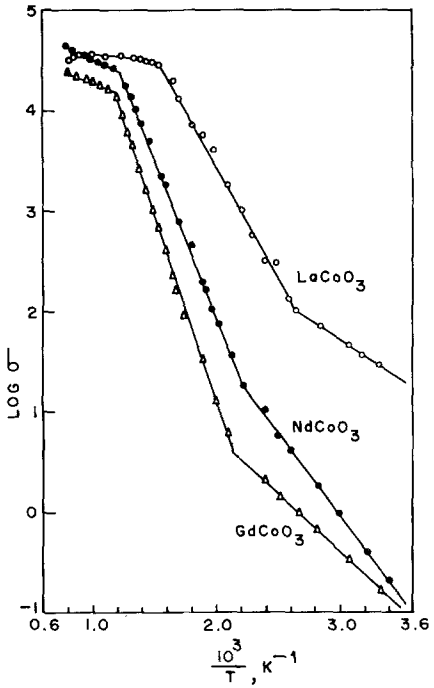

Fig. 2. Logarithmic of electrical conductivity σ (in $\Omega^{-1} \cdot m^{-1}$) of $NdCoO_3$, $GdCoO_3$, and $LaCoO_3$ versus inverse temperature.

The values of ΔE obtained from these expressions in the respective temperature ranges are given in Table III. These values were used in subsequent calculations.

Table III. Activation Energy for Electrical Conduction in $NdCoO_3$ and $GdCoO_3$

Sample	Temperature range (K)	ΔE (eV)
$NdCoO_3$	300–450	0.33
	450–800	0.63
	800–1250	0.11
$GdCoO_3$	300–450	0.23
	450–850	0.74
	850–1250	0.09

4. DISCUSSION

The total thermal conductivity of a solid is given by summing up the contributions from the different modes of thermal conduction and generally expressed as

$$\lambda = \sum_i \lambda_i \tag{9}$$

where i denotes the particular conduction mode and λ is the total conductivity. In the case of a semiconducting solid, the different modes are those arising mainly from electronic (λ_e), phononic (λ_p), and ambipolar (λ_{amb}) conduction. Thus Eq. (9) can be rewritten as

$$\lambda = \lambda_e + \lambda_p + \lambda_{amb} \tag{10}$$

Since the estimated radiative thermal conductivity of these oxides was found to be quite insignificant in the temperature range of our investigations, its contribution has not been considered in the above expression. In the equation it is of interest to note that none of the terms involved has any exponential dependence of the observed magnitude on temperature. Hence in order to explain the measured conductivity data it is necessary to include the excitonic contribution (λ_{ex}) in Eq. (10), i.e., λ for these oxides is given as

$$\lambda = \lambda_e + \lambda_p + \lambda_{amb} + \lambda_{ex} \tag{11}$$

λ_{ex} has been obtained from Eq. (11) by the usual method of subtracting the sum of the other components from the total measured conductivity. The method employed for calculating them is described below and the values thus obtained are given in Table IV.

The electronic part of the thermal conductivity (λ_e) of the oxides is calculated using the Wiedmann Franz Lorenz relation

$$\lambda_e = L\sigma T \tag{12}$$

where L is the Lorenz number, σ is the electrical conductivity, and T is the absolute temperature. It was Fine and Hsieh [21] and Morgan [22] who confirmed the validity of this relation in calculating the electronic thermal conductivity arising from free electrons and holes in semiconducting oxides and other ceramics. Subsequently this relation has been widely employed for such calculations. The λ_e thus obtained from the measured electrical conductivity data (given in Table IV) is not significant compared to the measured thermal conductivity throughout the temperature range.

Although various expressions describing the linear dependence of λ_p, with inverse temperature, are available for calculating the phononic

Table IV. The Calculated Electronic (λ_e), Phonic (λ_p), Ambipolar (λ_{amb}), and Excitonic (λ_{ex}) Thermal Conductivity of $NdCoO_3$ and $GdCoO_3$ (in $W \cdot m^{-1} \cdot K^{-1}$)

	$NdCoO_3$				$GdCoO_3$		
Temp. (K)	λ_e	λ_p	λ_{amb}	λ_{ex}	λ_e	λ_{amb}	λ_{ex}
350	1.40×10^{-5}	2.82	6.15×10^{-5}	0.78	7.79×10^{-6}	1.31×10^{-5}	0.88
400	6.24×10^{-5}	2.46	2.28×10^{-4}	1.34	1.46×10^{-6}	3.22×10^{-5}	1.54
450	2.06×10^{-4}	2.18	1.65×10^{-3}	2.02	3.40×10^{-5}	6.48×10^{-5}	2.00
500	1.15×10^{-3}	1.97	7.82×10^{-3}	2.73	1.55×10^{-4}	5.73×10^{-4}	2.83
550	4.76×10^{-3}	1.78	2.78×10^{-2}	3.44	8.10×10^{-4}	6.18×10^{-3}	3.62
600	1.56×10^{-2}	1.65	8.00×10^{-2}	4.10	3.25×10^{-3}	2.16×10^{-2}	4.36
650	4.30×10^{-2}	1.51	1.95×10^{-1}	4.75	1.06×10^{-2}	6.23×10^{-2}	5.22
700	1.02×10^{-1}	1.40	4.20×10^{-1}	5.23	2.94×10^{-2}	1.54×10^{-1}	5.72
800	4.29×10^{-1}	1.23	2.66×10^{-1}	6.62	1.56×10^{-1}	6.72×10^{-1}	6.84
900	6.10×10^{-1}	1.09	3.51×10^{-1}	7.95	3.77×10^{-1}	1.96×10^{-1}	8.43
950	6.90×10^{-1}	1.03	3.88×10^{-1}	8.69	4.23×10^{-1}	2.15×10^{-1}	9.13
1000	7.72×10^{-1}	0.98	4.26×10^{-1}	9.32	4.70×10^{-1}	2.34×10^{-1}	9.02
1050	8.61×10^{-1}	0.94	4.64×10^{-1}	9.34	5.18×10^{-1}	2.53×10^{-1}	8.09
1100	9.60×10^{-1}	0.89	5.03×10^{-1}	8.65	5.67×10^{-1}	2.72×10^{-1}	7.16
1150	1.05	0.86	5.43×10^{-1}	7.05	6.18×10^{-1}	2.92×10^{-1}	6.18

conduction, the resulting data are seldom found to be in agreement with λ_p observed experimentally [23, 24]. In order to overcome this difficulty, λ_p was estimated by the extrapolation method. The phononic thermal conductivity (λ_p) of $NdCoO_3$ is obtained by extrapolating the low-temprature (below 300 K) data of Gerthsen and Kettle [13] after applying the porosity correction as mentioned previously. These extrapolated values of λ_p are ~ 63 and 8% of the measured conductivities at 400 and 1000 K, respectively, as can be seen from the data given in Table IV. Since both $NdCoO_3$ and $GdCoO_3$ have the same crystal structure, similar thermophysical properties, and also nearly the same thermal conductivity, λ_p of the latter was assumed to be same as that of $NdCoO_3$.

Ambipolar thermal conduction (λ_{amb}) results from the simultaneous drifting of electrons and holes along the temperature gradient, where they partly recombine and release their formation energy, thus contributing significantly to the thermal conductivity. This mode of heat conduction is prevalent in intrinsic semiconductors [25, 26]. The λ_{amb} is evaluated using the expression [27]

$$\lambda_{amb} = \sigma T \left(\frac{k}{e}\right)^2 \frac{b}{(1+b)^2} \left(\frac{\Delta E}{kT} + 4\right)^2 \tag{13}$$

where b is the hole-to-electron mobility ratio, ΔE is the activation energy for electrical conduction, e is the electronic charge, and the other terms are as defined earlier. Gerthsen and Hardtl [28] reported a hole-to-electron mobility ratio of 13.5 for $LaCoO_3$ at room temperature and observed that the ratio is almost independent of the densities of charge carriers. Since the electrical conductivity and Seebeck coefficient [9, 11] of $LaCoO_3$, $NdCoO_3$, and $GdCoO_3$ are found to be characteristically similar, the mobility ratios for $NdCoO_3$ and $GdCoO_3$ are considered more or less the same as that of $LaCoO_3$. Using the measured electrical conductivity and the activation energy data (Table III), the ambipolar conductivity is calculated and given in Table IV. The maximum value of this is only 8% of the measured conductivity.

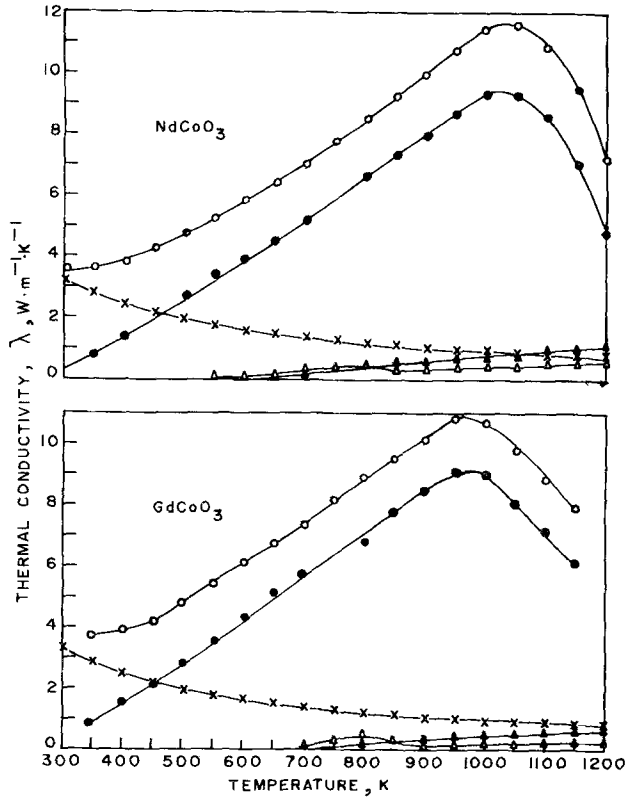

Fig. 3. Measured thermal conductivity (○) and the calculated phononic (×), electronic (▲), ambipolar (△), and excitonic (●) thermal conductivities of $NdCoO_3$ and $GdCoO_3$ as a function of temperature.

Having calculated λ_e, λ_p, and λ_{amb}, their sum is found to be much less than the measured conductivity in both compounds, and as stated above the difference arises due to the excitonic contribution. The λ_{ex} obtained using Eq. (11), along with the other components, λ_e, λ_p, λ_{amb}, and the total measured thermal conductivity, for $NdCoO_3$ and $GdCoO_3$ are shown in Fig. 3 as a function of temperature up to 1200 K. The plot of log λ_{ex} versus the inverse of temperature is given in Fig. 4, which clearly shows the exponential dependence of λ_{ex} over T in the semiconducting phase.

Pikus [4], as stated earlier, deduced a theoretical expression to describe the excitonic thermal conduction in solids following the assumption that the mean free path of exciton does not depend on its energy. The equation can be expressed as [2, 29]

$$\lambda_{ex} = \frac{16}{3}\pi\left(\frac{k}{h}\right)^3 l\mu T^2\left[\left(\frac{\varepsilon}{kT}+2\right)^2+2\right]\exp\left(-\frac{\varepsilon}{kT}\right) \tag{14}$$

where ε is the energy of formation of the exciton, l is its mean free path, μ is its effective mass, h is the Planck constant, and the other terms are as

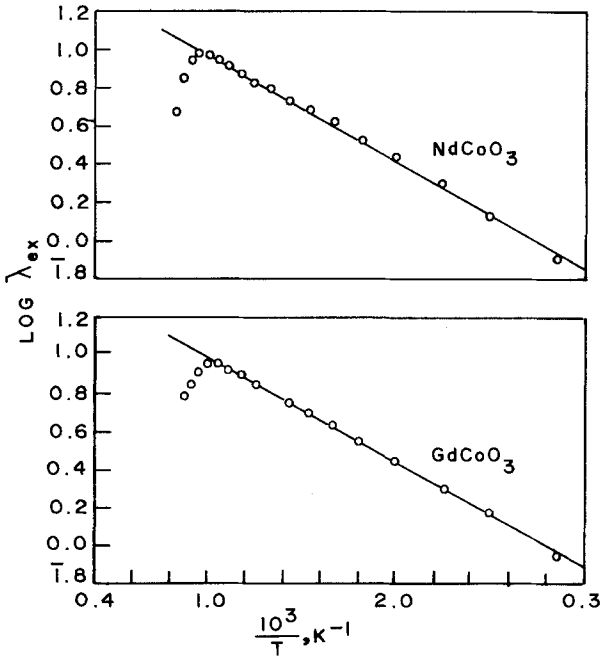

Fig. 4. Logarithm of calculated excitonic thermal conductivity (in $W \cdot m^{-1} \cdot K^{-1}$) of $NdCoO_3$ and $GdCoO_3$ versus inverse temperature.

defined earlier. In Eq. (14), since the exponential term predominates over all the other terms, it can be approximated as [13, 29]

$$\lambda_{ex} = A \exp(-\varepsilon/kT) \tag{15}$$

where A is a constant incorporating all the other terms of Eq. (14). Equation (15) defines the exponential dependence of λ_{ex} on T as revealed by the experimental results shown in Fig. 4. The values of A and ε calculated by fitting the λ_{ex} data in Eq. (15) are given in Table V. It is interesting to note that the observed energy of formation of exciton in both the compounds is the same as that of $LaCoO_3$ [15, 16] and is in good agreement with the activation energy 0.1 eV reported as the t_{2g}–e_g energy gap from the electrical conductivity data of $LaCoO_3$ [8]. This close agreement in energy values gives support to the excitonic mode of thermal conduction in these oxides, where an exciton is formed by coupling an e_g electron with at t_{2g} hole in the cobalt ion [7].

As the semiconducting oxides undergo transition to metals, the finite energy gap responsible for their high semiconductivity and exciton formation is progressively reduced, and as the oxides become metals, the energy gap and the exciton density would drop to zero, leading to a corresponding drop in the excitonic thermal conductivity. The plots of log σ versus $1/T$ for both these oxides show a change of slope at around 450 and 850 K (Fig. 2). This behavior in electrical conductivity is almost identical to that observed by Rajoria et al. [9]. From their data on the DTA, Debye–Waller factor, and Seebeck coefficient, the authors showed that these oxides undergo a second-order transition in the temperature region of 400–600 K and a first-order electronic transition at 1030 and 970 K, respectively, for $NdCoO_3$ and $GdCoO_3$. The thermal conductivity data do not show any variation in the low-temperature region. However, the conductivity reaches a broad maximum at 1030 K for $NdCoO_3$ and at 975 K for $GdCoO_3$; thereafter, the conductivity decreases rapidly. A similar behavior is observed for $LaCoO_3$, where the maximum coincides with its semiconductor-to-metal transition temperature of 1210 K.

Table V. Calculated A and ε Values of $NdCoO_3$ and $GdCoO_3$

Sample	A ($W \cdot m^{-1} \cdot K^{-1}$)	ε (eV)
$NdCoO_3$	33.75	0.11
$GdCoO_3$	35.27	0.11

5. CONCLUSIONS

The thermal conductivity of $NdCoO_3$ and $GdCoO_3$ is predominantly excitonic at high temperatures as in the case of $LaCoO_3$. The estimated formation energy of excitons from the thermal conductivity data is found to be the same as the reported energy difference between the e_g and the t_{2g} energy levels of the cobalt ions. This energy match substantiates that the exciton formation is due to the e_g–t_{2g} electron hole pair coupling in the oxides.

ACKNOWLEDGMENT

The authors thank Dr. R. P. Agarwala, Head, Material Science Section, for his valuable guidance and discussions.

REFERENCES

1. G. Busch and Schneider, *Physica* **20**:1084 (1954).
2. A. F. Joffe, *Can. J. Phys.* **34**:1342 (1956).
3. E. D. Devyatkova, *Sovit. Phys. Tech. Phys.* **2**:414 (1957).
4. G. E. Pikus, *Sovit. Phys. Tech. Phys.* **1**:32 (1957).
5. J. B. Goodenough, *Czech. J. Phys.* **17B**:304 (1967).
6. C. N. R. Rao and K. J. Rao, *Phase Transitions in Solids* (McGraw–Hill, New York, 1978).
7. P. M. Raccah and J. B. Goodenough, *Phys. Rev.* **155**:932 (1967).
8. V. G. Bhide, D. S. Rajoria, G. Rama Rao, and C. N. R. Rao, *Phys. Rev.* **6B**:1021 (1972).
9. D. S. Rajoria, V. G. Bhide, G. Rama Rao, and C. N. R. Rao, *J. Chem. Soc. Faraday Trans. II* **70**:512 (1974).
10. G. Thornton, B. C. Tofield, and D. E. Williams, *Solid State Commun.* **44**:1213 (1982).
11. A. Casalot, P. Dougier, and P. Hagenmuller, *J. Phys. Chem. Solids* **32**:407 (1971).
12. R. A. Bari and J. Sivardiere, *Phys. Rev.* **B5**:4466 (1972).
13. P. Gerthsen and F. Kettle, *J. Phys. Chem. Solids* **25**:1023 (1964).
14. C. G. S. Pillai and A. M. George, *Int. J. Thermophys.* **4**(2):183 (1983).
15. C. G. S. Pillai and A. M. George, *Proc. Ind. Nat. Sci. Acad.* **54A**:824 (1988).
16. C. G. S. Pillai, Ph.D. thesis (Bombay University, Bombay, 1987).
17. C. G. S. Pillai and A. M. George, Report BARC-1122 (1981).
18. V. V. Mirkovich, *J. Am. Ceram. Soc.* **48**:387 (1965).
19. A. M. George and I. K. Gopalakrishnan, *J. Phys. E. Sci. Instr.* **8**:13 (1975).
20. J. Francl and W. D. Kingery, *J. Am. Ceram. Soc.* **37**:99 (1954).
21. M. E. Fine and N. Hsieh, *J. Am. Ceram. Soc.* **57**:502 (1974).
22. P. E. D. Morgan, *J. Am. Ceram. Soc.* **58**:349 (1975).
23. R. Roufosse and P. G. Klemens, *Phys. Rev.* **7B**:5379 (1973).
24. G. A. Slack, in *Solid State Physics*, H. Ehrenrich, F. Seitz, and D. Turnbull, eds., (Academic Press, New York, 1979), Vol. 34, p. 1.

25. P. J. Price, *Phil. Mag.* **46**:422 (1955).
26. C. J. Glassbrenner and G. A. Slack, *Phys. Rev.* **134A**:1058 (1964).
27. J. E. Parrott and A. D. Stuckes, *Thermal Conductivity of Solids* (Pion, London, 1975).
28. P. Gerthsen and K. H. Hardtl, *Z. Naturf.* **17a**:514 (1962).
29. E. A. Lubimova, in *The Earth's Mantle*, T. F. Gaskell, ed. (Academic Press, London, 1967), pp. 253–271.

Printed in Belgium